JOURNAL OF AIRCRAFT
Vol. 39, No. 4, July–August 2002

Helicopter Flight Dynamic Simulation with Refined Aerodynamics and Flexible Blade Modeling

Colin Theodore* and Roberto Celi†
University of Maryland, College Park, Maryland 20742-3015

A coupled rotor–fuselage flight dynamic model that includes a maneuvering free wake model and a coupled flap–lag–torsion flexible blade model, as well as the results of an investigation on some effects of inflow and blade modeling on the free-flight response of a hingeless rotor helicopter to pilot inputs, are described. The wake model is a relaxation type free wake, capable of modeling the wake geometry changes due to maneuvers; no assumptions are made on the wake geometry, which is free to evolve based on the maneuver. Theoretical predictions are compared with flight-test data. The results show that the free-flight, on-axis response to pilot pitch and roll inputs can be predicted with good accuracy with a relatively unsophisticated model. It is possible to predict the off-axis response from first principles, that is, without empirically derived correction factors and without assumptions on the wake geometry. To do so, however, requires sophisticated modeling. Both a free wake model that includes the wake distortions caused by the maneuver and a refined flexible blade model must be used. Most features of the off-axis response can be captured using a dynamic inflow theory extended to account for maneuver-induced wake distortions, for a fraction of the cost of using a free wake model. The most cost-effective strategy, for typical flight dynamic analyses and if vibratory loads are not required, is probably to calibrate such a theory using the more accurate free wake based model, and then use it in all calculations.

Nomenclature

p, q, r	=	roll, pitch, and yaw rates of the helicopter
t	=	time, s
u, v, w	=	helicopter velocity components along the body axes
$\boldsymbol{u}$	=	control vector
$\boldsymbol{y}$	=	state vector
Δt	=	integration time step, s
$\Delta\zeta$	=	resolution of the vortex filament discretization, deg
$\zeta_{\max}$	=	length of vortex filaments, deg

Introduction

IN recent years, the need for a reliable design of flight control systems has prompted interest in improving the accuracy of flight dynamic mathematical models of helicopters. In particular, this has led to a more sophisticated modeling of the rotor system, both from the dynamic and the aerodynamic points of view. Much research has been devoted to one long standing problem in flight dynamic modeling, namely, the prediction of the off-axis response to pilot input, and especially of pitch and roll cross coupling. Until recently, the predictions of the off-axis response, for example, the pitch response to a lateral cyclic pitch input, were inaccurate, to the point of sometimes having the wrong sign, compared to the results of flight tests. The cause for the discrepancies has eluded the helicopter flight dynamics community for many years.

The first major contribution to the understanding of the off-axis response problem has come from the work of Rosen and Isser,[1,2] who were the first to point out the importance of vortex spacing on the inflow distribution over the rotor disk during steady pitch and roll maneuvers. Pitch and roll angular rates change the vertical spacing of the wake vortices by reducing the spacing on one side of the rotor disk and increasing the spacing on the opposite side. This change in wake geometry modifies the inflow distribution at the rotor disk, which redistributes the aerodynamic loads on the rotor. This causes changes in the blade flapping response and, in turn, changes the rotor pitch and roll moments. When these geometry changes were taken into account through a specially developed prescribed wake model, the prediction of cross-coupling pitch and roll derivatives for the UH-60 and AH-64 helicopters were improved. The most visible sign of the improvement brought about by the inclusion of the wake distortion effects was the change of the sign of the lateral flapping response due to a steady pitching motion of the shaft.

Following Rosen and Isser's work,[1,2] other investigators have proposed simpler, momentum-based inflow models that capture the inflow changes due to a maneuver through the use of correction coefficients. Keller[3] and Keller and Curtiss[4] and Arnold et al.[5] have developed an extended momentum theory that includes simple additional inflow terms proportional to pitch and roll rates. The additional terms are characterized by the use of correction coefficients, the numerical values of which are determined based on a simplified vortex wake analysis that is specialized for hovering flight. Significant improvements were obtained for the prediction of the off-axis response of the UH-60 in hover. The wake geometry changes due to a maneuver have also been modeled by Basset and Tchen-Fo,[6] who used a dynamic vortex wake model with the wake being represented by sets of vortex rings, the positions, geometry, and vorticity of which evolve dynamically as a function of the rotor airloads, inflow, and rotor motion. Correction coefficients (such as those used by Keller[3]) were reconstructed from the inflow perturbations due to maneuvers both in hover and forward flight conditions. Substantial improvements in the predictions of the hover off-axis response for the BO-105 were obtained. The variation in the wake distortion correction coefficients with advance ratio was also investigated. The popular dynamic inflow model has also been extended to capture the effects of maneuver-induced wake distortions by Krothapalli et al.[7,8]

A completely different explanation for the discrepancies of off-axis response predictions has been offered by von Grünhagen.[9] The off-axis agreement can be improved by including a virtual inertia effect associated with the downwash swirl in the rotor wake. This virtual inertia of the wake essentially adds to the angular momentum of the rotor and produces additional moments during pitch and roll maneuvers. This results in simple correction terms that are added

Received 5 March 2000; revision received 17 January 2002; accepted for publication 26 March 2002.

*Graduate Research Assistant, Alfred Gessow Rotorcraft Center, Department of Aerospace Engineering. Student Member AIAA.

†Associate Professor, Alfred Gessow Rotorcraft Center, Department of Aerospace Engineering. Member AIAA.

to the overall pitch and roll moment equilibrium equations of the helicopter and that improve considerably the off-axis predictions for a BO-105 both in hover and forward flight.

All of the previous studies attempt to improve the correlation of off-axis response through refined theoretical models. A different approach has been proposed by Mansur and Tischler,[10] based on test data. Corrected lift and drag coefficients of the blade airfoils are obtained from the instantaneous, baseline values through a first-order filter, the time constant of which is selected in terms of an equivalent aerodynamic phase lag. This phase lag is then determined using system identification techniques from flight-test data or, more recently, from simulated flight-test data based on the Rosen et al. prescribed wake model.[11]

A free wake model that can capture the wake distortions due to pitch and roll rates has been recently developed by Bagai et al.[12] for one or more isolated rotors. The most important feature of this wake model is that no a priori assumptions are required for the wake geometry. The geometry is determined by the convection of the vortex filaments in the induced velocity field and takes rigorously into account the kinematics of the maneuver. Although the vortex model is quite general, and a lattice of shed and trailed vorticity could be generated, the wake was typically represented with just blade tip vortices. Subsequently, Park and Leishman investigated the effects of unsteady aerodynamics on the rotor wake behavior in maneuvers.[13] Four models of increasing complexity were used: tip vortex only and quasi-steady aerodynamics (the baseline case), tip vortex only and blade element type unsteady aerodynamics based on an indicial model, quasi-steady aerodynamics and multiple trailed vortices, and a complete lattice of trailed and shed vortices. The study concluded that wake geometry and inflow predictions are not very sensitive to unsteady aerodynamic effects, and the trailed vorticity remains the most important contributor.

In light of the research just described, the general objective of the present study is to determine whether it is possible to simulate accurately the response of a helicopter from a mathematical model based on first principles, that is, without empirically derived correction factors and without a priori assumptions on the wake geometry.

The specific objectives of the paper are as follows:

1) To describe a nonreal-time flight dynamic simulation model that includes both blade flexibility, with coupled flap, lag, and torsion degrees of freedom, and the maneuvering free wake model of Ref. 12.

2) To use this refined model to investigate the effects of inflow and blade modeling on the free-flight response of the BO-105 helicopter in a near hover maneuver, including comparisons with flight-test data.

3) To compare the predictions of the free-wake based model with those obtained using one of the simpler, momentum-based models, namely, that of Keller and Curtiss.[4]

Mathematical Model

Flight Dynamic Model

The flight dynamic model is described in detail in Refs. 14–16, and only a brief summary of its main features will be presented here. The simulation model is based on a set of coupled nonlinear rotor–fuselage equations in first-order, state-space form. The rigid-body dynamics of the helicopter are modeled using nonlinear Euler equations. The aerodynamic characteristics of the fuselage and of the horizontal and vertical tail are provided in the form of look-up tables as a function of angle of attack and sideslip, which need not be small angles.

The rotor model describes the dynamics of each blade with coupled flap, lag, and torsion degrees of freedom. A finite element formulation is used to model the blade, coupled with a modal coordinate transformation to reduce the number of degree of freedom and, therefore, the number of equations describing the blade dynamics. The blade equations are written to take into account arbitrary hub motions; the blade elastic deformations need not be small. With a combination of the rigid-body fuselage equations with the blade dynamics equations, the result is a system of first-order coupled differential equations for the rotor and fuselage. Quasi-steady aerodynamics are used to calculate the aerodynamic loads; the aerodynamic coefficients of the blade airfoil are provided in the form of look-up tables as a function of angle of attack and Mach number. Main rotor inflow is calculated using a maneuvering free wake model,[12] a three-state dynamic inflow model[17] without maneuver wake corrections, or an extended momentum theory that does include maneuver corrections.[3,4] When a free wake is not used, tip losses are approximately taken into account by assuming that the outboard 3% of the blade does not generate aerodynamic loads. A one-state dynamic inflow model is used for the tail rotor.

Maneuvering Free Wake Model

The free wake model coupled with the flight dynamic code is the Bagai-Leishman free wake model.[12] The main characteristic of this free wake model from the point of view of a flight dynamic simulation is that it can model distortions of the wake geometry caused by a maneuver. The wake is discretized into a number of straight line vortex segments that together describe the geometry of the wake. The number of straight line vortex segments used for each rotor blade is determined by two parameters, namely, the vortex filament discretization resolution $\Delta\zeta$, measured in degrees, and the total length of the trailed vortex considered in the analysis. This length, also measured in degrees, is given by the number of rotor revolutions from the time that the filament was first generated, is prescribed by the user, and can be interpreted as a measure of the total wake age.

The bound circulation is an input to the free wake code and is given at a number of radial blade segments at each azimuth angle considered. The number of blade segments is arbitrary; they do not have to be of equal length along the span. The bound circulation is assumed to be constant over each blade segment. Note that the free wake code used in this analysis can model multiple trailed vortices, to be released along the span of the blade, but only a single trailed tip vortex per blade is used in this study.

The calculation of the wake geometry is performed using a pseudo-implicit predictor–corrector numerical method.[18] An iterative process is involved in calculating the rotor wake geometry for a given bound circulation distribution. An initial wake geometry is used to start the iterative process. With each iteration, the geometry of the free wake is changed according to the pseudo-implicit predictor–corrector equations so that a new wake geometry is generated. The convergence criteria for the wake geometry is based on the L_2 norm of the change in wake geometry between successive iterations.[18]

The converged wake is used to calculate the local induced velocity at specified points along the blades and around the azimuth. These local velocities only contain contributions from the bound and wake circulations and represent only the induced velocity. The freestream and maneuver velocity contributions are provided by the flight dynamic code.

Free-Flight Response Calculation

Coupling of Flight Dynamic and Free Wake Models

The maneuvering free wake was developed for one or more isolated rotors. However, the theory contains all of the modeling ingredients required for use in a complete helicopter simulation. Coupling the flight dynamic and the free wake models requires some transformations and minor reformulations so that the two models interact in a consistent manner. For example, the flight dynamic model uses a body-fixed coordinate system for the fuselage equations and a rotating, undeformed blade coordinate system for the rotor blade equations. The free wake model, on the other hand, is formulated in a wind axis coordinate system. The details of the coupling of the two formulations are omitted here for brevity and can be found in Ref. 19.

The flight dynamic model provides several inputs to the free wake model, as follows:

1) *Circulation distribution.* This is the spanwise and azimuthwise distribution of bound circulation, and is calculated in the

aerodynamic portion of the flight dynamic code. At a given blade azimuth, the wake model selects as the initial strength of the tip vortex the maximum value of the bound circulation along the blade at that azimuth.

2) *Rigid blade flapping angles.* The free wake model makes the assumption that the blade is rigid. This is not a critical assumption from an aerodynamic point of view, and it could easily be removed; however, it was maintained in this study. The flapping angles are used to determine the displacements of the tips of each blade, which are the release points of the individual vortex filaments. Because in the flight dynamic analysis the blade can be flexible, an equivalent rigid flapping angle is defined, at each azimuth angle, as the flapping angle of a straight blade, hinged in flap at the axis of rotation, that has the same tip flap deflection as the elastic blade.

3) *Hub linear and angular velocities.* The linear and angular velocities of the fuselage are transformed to the wake coordinate system, and used to define the external velocity profile that is applied to the free wake geometry.

Baseline Response Procedure

The calculation of time histories using the flight dynamic model involves the direct numerical integration of the equations of motion with respect to time, from a given initial condition. In this case, the starting point is the trim condition at which the time histories are to be calculated. The basic trim procedure used in this study is essentially the same as that described in Refs. 20 and 21. This is a coupled rotor–fuselage trim procedure for a helicopter in a steady coordinated helical turn; straight and level flight is considered as a special case of turn with zero turn rate and flight-path angle. It can be characterized as an algebraic trim procedure because the trim problem is defined by a set of coupled nonlinear algebraic equations.[20,22]

Because the equations of motion are formulated as a system of first-order, nonlinear, ordinary differential equations, $\dot{\boldsymbol{y}} = \boldsymbol{f}(\boldsymbol{y}, \boldsymbol{u}; t)$, a conventional ordinary differential equation (ODE) solver can be used to integrate the equations numerically. For this study, the variable step, variable order Adams–Bashforth ODE solver (DE/STEP) is used for the numerical integration. The integration is carried out from trim, and the time history is calculated for a prescribed set of control inputs.

Response Procedure with Free Wake Model

The calculation of time histories first requires the trim solution for the given flight condition. The trim procedure with the free wake model is detailed in Refs. 19 and 23.

With the inclusion of the free wake model, the equations of motion no longer include equations for the main rotor inflow dynamics, and the state vector $\boldsymbol{y}$ no longer includes inflow information. In this case, the free wake model is used to provide the main rotor inflow. With the exception of the treatment of the free wake, the time integration procedure is similar to the baseline procedure, and the same ODE solver is used to integrate the equations of motion.

The free wake model used in this study is a steady-state model that is based on a relaxation technique. As such, it is strictly valid only in steady-state conditions, and it cannot be rigorously used in a time-marching procedure. The general idea for coupling wake calculations and ODE solutions is then to calculate wake geometry and inflow distribution at the end of each rotor revolution and to keep geometry and inflow constant over the next revolution.

For a more precise description, consider first the general structure of wake calculations shown in Fig. 1. The structure is that of a double-nested loop. For a given helicopter state, the circulation loop is started by assuming an initial inflow distribution. For the response calculations, the initial inflow distribution is the final solution from the previous rotor revolution. Note that, in Fig. 1, the blade motions and linear and angular velocities of the fuselage are not explicitly a part of this iterative process because they are held fixed during the calculation of bound circulation, wake geometry, and inflow. The initial inflow distribution is used in the flight dynamic code to calculate the blade loading, including the bound circulation distribution over the rotor disk. The circulation is supplied to the free

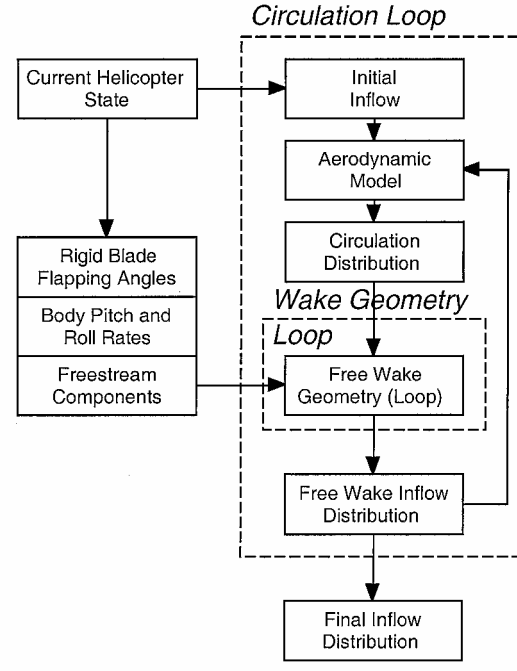

Fig. 1 Schematic of coupling of circulation and geometry loops to the flight dynamic code.

wake model, which iterates on the wake geometry and produces an updated inflow distribution when the wake has converged. The updated inflow is then used in the flight dynamic code to calculate an updated bound circulation distribution, which is fed again into the wake, to calculate a new geometry and a new inflow. This loop is considered converged when the change in inflow between successive iterations falls below a given tolerance.

With this in mind, the free-flight response calculations proceed as follows:

1) The procedure starts from the trimmed flight condition, represented by $\boldsymbol{y}(t = 0)$ and the trimmed control settings $\boldsymbol{u}(t = 0)$. The trim calculations also provide a free wake based, converged, trim inflow distribution.

2) The inflow distribution is held fixed, and the equations of motion are integrated for one rotor revolution using the desired control positions. During this integration, changes in the control positions and corresponding changes in the helicopter state vector do not affect the wake geometry and inflow distribution.

3) At the end of the rotor revolution, the helicopter state $\boldsymbol{y}$ (which describes the rotor blade motion and the linear and angular velocities of the fuselage) and control positions $\boldsymbol{u}$ are used to evaluate the circulation loop (Fig. 1). States, controls, and circulation at the end of the revolution are provided as input to the free wake, which updates geometry and inflow distribution as if states and controls were constant and not time dependent.

4) Steps 2 and 3 are repeated until the simulation is complete.

Results

The results presented in this section refer to a Eurocopter BO-105 helicopter with the flight control system turned off (bare airframe configuration). The BO-105 has a hingeless soft in-plane main rotor. This configuration results in an equivalent hinge offset of about 14%, which produces a high control power and bandwidth, making the helicopter highly maneuverable. The high equivalent hinge offset also contributes to high cross couplings between the longitudinal and lateral–directional dynamics of the helicopter.

The main rotor blades are modeled at two levels of sophistication. In the simpler blade model, only the first flap bending mode is used to model the rotor blade flexibility; in the more refined model, the seven lowest frequency elastic modes are used. In the calculations of the normal modes, the geometric pitch angle at the root of the blade is set to zero. The cross-sectional centers of gravity and shear of the blade are coincident at the quarter-chord location, which effectively

Table 1 BO-105 blade natural frequencies

Mode	Frequency, revolutions^{-1} Present study	Ref. 26	Mode type
1	1.1253	1.125	First flap
2	0.7316	0.732	First lag
3	3.1806	3.176	First torsion
4	3.4141	2.780	Second flap
5	4.4860	4.510	Second lag
6	7.6743	5.007	Third flap
7	9.1375	6.349	Second torsion

decouples torsion from the flap and lag degrees of freedom when considering the structural and inertial contributions. The presence of the small amount of structural twist of the blade introduces a small coupling between the flap and lag bending modes. Four finite elements of equal spanwise length are used in all blade models. The mass and stiffness distributions of the blade are assumed to be uniform for the current study, and their values are chosen so that the fundamental flap, lag, and torsion frequencies match those presented in Ref. 25. Table 1 lists the modes that are included in the current analysis, including the modal natural frequencies for the current analysis and those from Ref. 25 (which are based on the true, nonuniform mass and stiffness distributions) and the type of the mode.

All of the results presented in this paper are for the free-flight response of the BO-105 in a near hover flight condition, namely, at a forward speed of 17 kn, an altitude of 250 ft, and a gross weight of 4850 lb. This corresponds to the flight conditions of the test flights described in Ref. 26. Pressure and density are those corresponding to the Standard Atmosphere. First, the stick fixed time history responses are presented, followed by the time history responses to a lateral cyclic pitch maneuver.

Stick Fixed Response

This section presents the results of a simulation with the controls held fixed at the calculated trim value. The purpose of the simulation is to determine the amount of drift from the trim conditions as a function of time: For a perfectly trimmed helicopter, all of the curves should either be straight lines or exactly periodic. The time history results are calculated with the dynamic inflow and free wake inflow models with the two main rotor blade configurations discussed earlier. All of the results are numerical.

Figures 2 and 3 show, respectively, the linear and angular accelerations at the center of gravity of the body as a function of time for the first 0.3 s of the time integration. This corresponds to about $2\frac{1}{4}$ rotor revolutions. Both the simple and refined blade models are used, with the simple blade model results being denoted by 1 mode and the refined blade model results with 7 modes. Figures 2 and 3 show the vibrational characteristics at the center of mass of the helicopter for each of the inflow and blade models. They also show show that the accelerations predicted using the free wake inflow model are at least an order of magnitude higher than those predicted using a momentum-theory-based dynamic inflow model.

With focus placed on the linear accelerations, Fig. 2 also shows that the magnitude of the vertical acceleration is higher than in the longitudinal and lateral directions; this is due to the higher main rotor loads in that direction. Figure 3 shows that the roll acceleration is higher than the pitch and yaw accelerations; this is because the roll inertia is lower than the pitch and yaw inertias. For the models that include the free wake, including coupled flap–lag–torsion dynamics (refined blade model) predicts higher vibrations at the center of gravity than the simpler blade model with the fundamental flap mode only.

The mathematical model of this study was not validated for vibratory load calculations. However, the general trends appear to be consistent with the results presented in Ref. 24, namely, that the predicted vibratory loads increase with the introduction of a free wake model and with a more sophisticated flexible blade modeling.

From a flight dynamic point of view, note that the predictions of the model with the free wake are not exactly periodic. Therefore, the

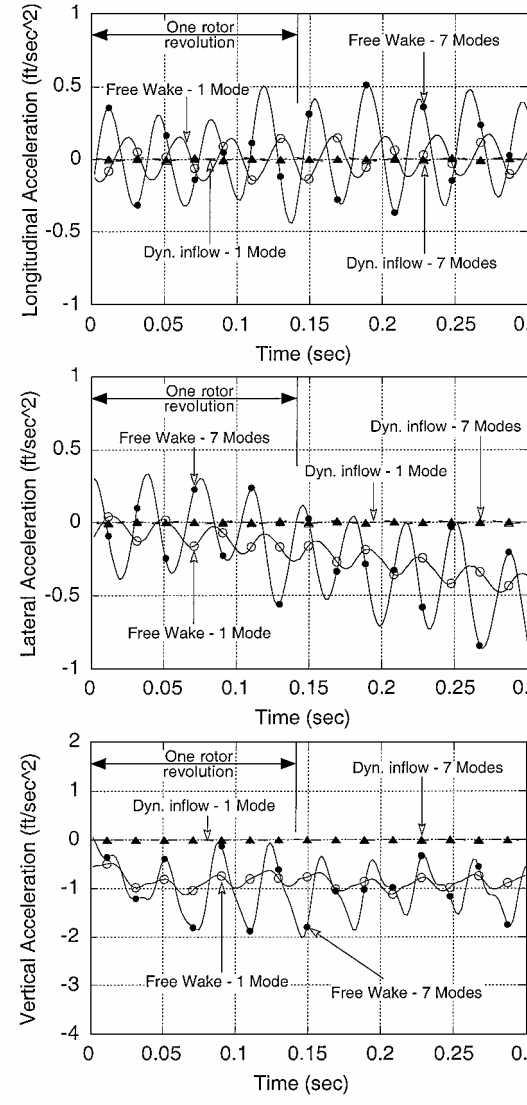

Fig. 2 Effect of inflow models and blade modeling on linear accelerations at the computed trim conditions.

average linear and angular accelerations of the aircraft are not equal to zero, and a slow drift away from trimmed conditions should be expected. Figures 4 and 5 show such a drift for the linear and angular velocities, respectively. The calculations were performed for 45 rotor revolutions, corresponding to just over 6 s of simulated time. The results obtained using the dynamic inflow model are also shown in Figs. 4 and 5. It is clearly seen in Figs. 4 and 5 that the linear and angular velocities calculated with the free wake model slowly deviate from trim, whereas the results with the dynamic inflow model remain almost perfectly trimmed. The deviations are larger with the refined blade model. The roll rate p (Fig. 5) calculated with the free wake and refined blade models builds up to 2–3 deg/s within the first few rotor revolutions. This is in part due to the higher angular accelerations in the roll direction with the free wake model and the refined blade model. All of the other linear and angular velocities build up more slowly.

The results of Figs. 4 and 5 indicate that the starting point for the integration is not an exact trim condition. The algebraic trim procedure used in the present analysis is based on the same mathematical model as the free-flight response simulation and does enforce, among other conditions, force and moment equilibrium on average over one rotor revolution. Furthermore, the linear and angular velocities are assumed to be constant. (The angular rates are assumed to be zero for straight flight.) This algebraic trim procedure does not, however, explicitly enforce periodicity of the states at the end of one revolution. Also, the time dependency of the blade

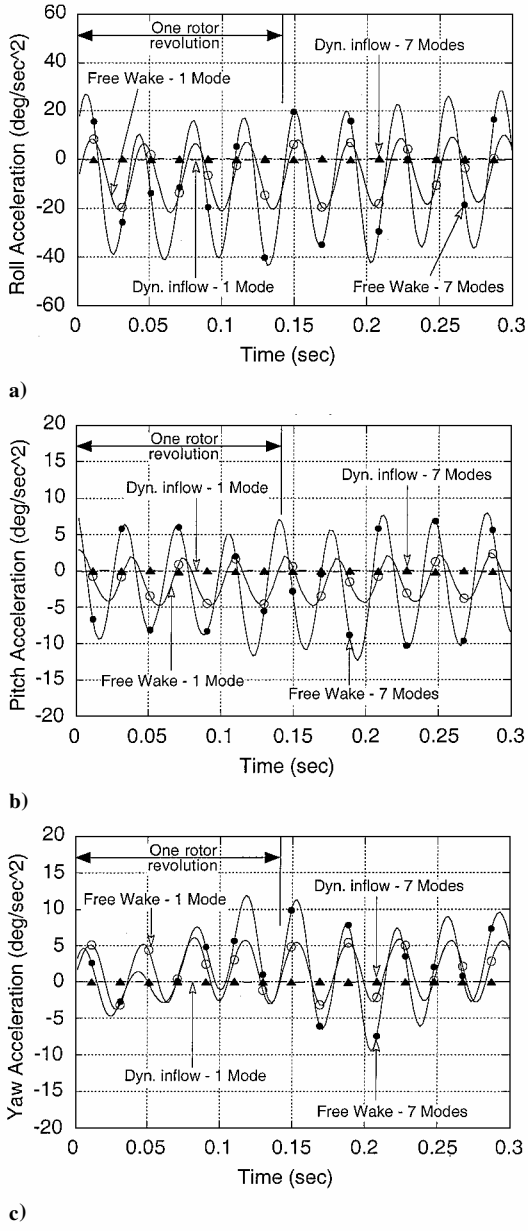

Fig. 3 Effect of inflow models and blade modeling on a) roll, b) pitch, and c) yaw accelerations at the computed trim conditions.

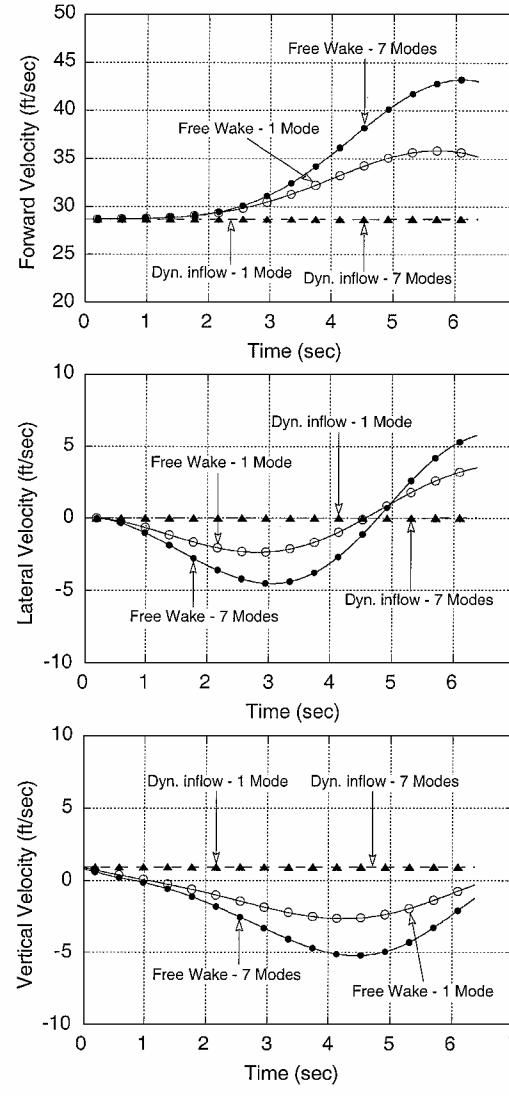

Fig. 4 Effect of inflow models and blade modeling on velocity components at the computed trim conditions.

motions is approximated in trim calculations by a truncated Fourier series, whereas the free-flight response calculations do not contain any such approximation. Therefore, there are small differences between the trim and the free-flight response solutions with fixed control, which result in the slow drift of the latter shown in Figs. 4 and 5.

This is not significant when the dynamic inflow model is used because the predicted accelerations are small. It only becomes an issue with the free wake model because of the higher predicted accelerations. An alternative to the algebraic trim is a periodic trim procedure that explicitly enforces periodicity. In a periodic trim condition, the helicopter returns to its original state after the equations of motion are integrated for each rotor revolution. This allows for the linear and angular velocities to vary through the time integration as long as they return to their original values after each rotor revolution. This procedure was described in Ref. 21, where it was called Phase II trim, and it was used to refine the results of an algebraic trim procedure (Phase I trim) identical to that used in the present study. In Ref. 21, no benefits were observed, but the results referred to an articulated, rigid blade, and dynamic inflow was used. A periodic trim procedure may be more appropriate when a free wake inflow model as well as blade flexible modes are used.

Free Flight Response to Lateral Maneuver

This section presents results of a free-flight simulation, for a mostly lateral cyclic maneuver at 17 kn. Simulation results for the BO-105 are compared with flight-test data. The control deflections that define the maneuver are shown in Fig. 6. The maneuver is part of a series of test flights carried out for system identification purposes[26]; the control excursions are relatively small, and the response of the helicopter is mostly in a linear range.

Figure 7 shows the roll and pitch rate predictions obtained using the dynamic inflow model, with the simple and refined blade models. The dynamic inflow model is the Pitt–Peters (see Ref. 17) three-state dynamic inflow model Ref. 17 that does not include the effect of maneuver on the wake geometry and, therefore, is representative of straight flight conditions only. The results show a typical trend, already observed by other investigators, namely, that the roll rate (on-axis) response is predicted accurately, whereas the pitch rate (off-axis) response is predicted poorly. The off-axis response predictions are not improved with the refined blade model that includes seven flexible blade modes.

Figure 8 shows the roll and pitch rate predictions obtained using the maneuvering free wake model with the simple and refined blade model. The results using the refined blade model with seven modes show that the on-axis response p is accurately predicted. The off-axis response q is also predicted with reasonable accuracy. The agreement for the initial pitch acceleration, which is indicated by the slope of the pitch rate response for t of about 1.5 s, is excellent; the same is true for t of about 3 s, when the helicopter responds

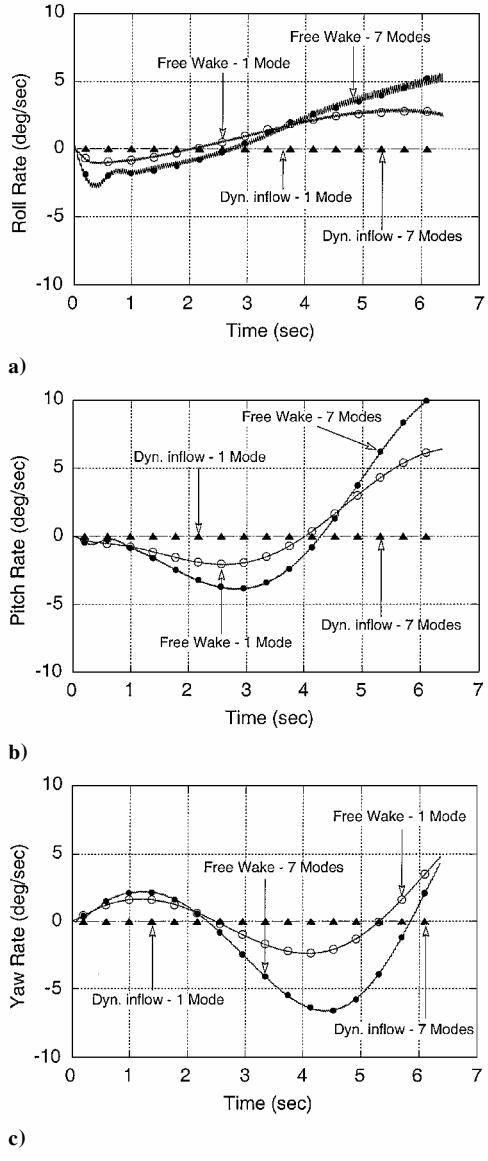

Fig. 5 Effect of inflow models and blade modeling on a) roll, b) pitch, and c) yaw rates at the computed trim conditions.

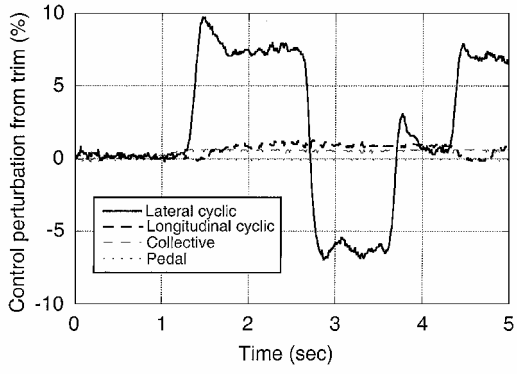

Fig. 6 Control deflections from trim for the selected maneuver, $V = 17$ kn.

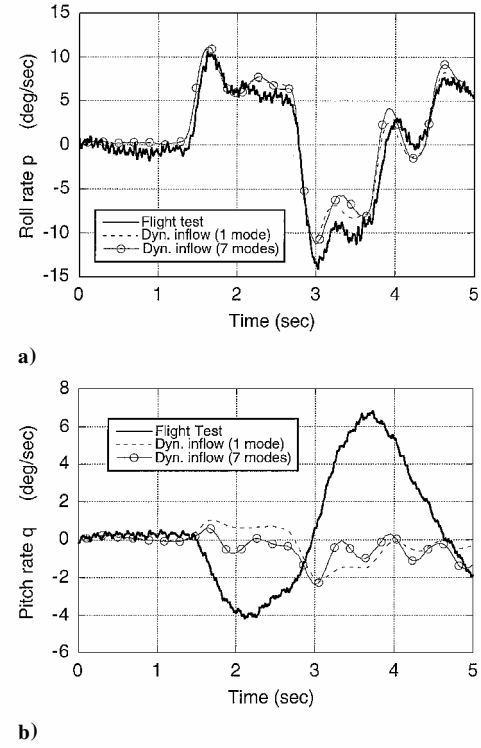

Fig. 7 Effect of number of modes on the a) roll and b) pitch rate response; dynamic inflow model.

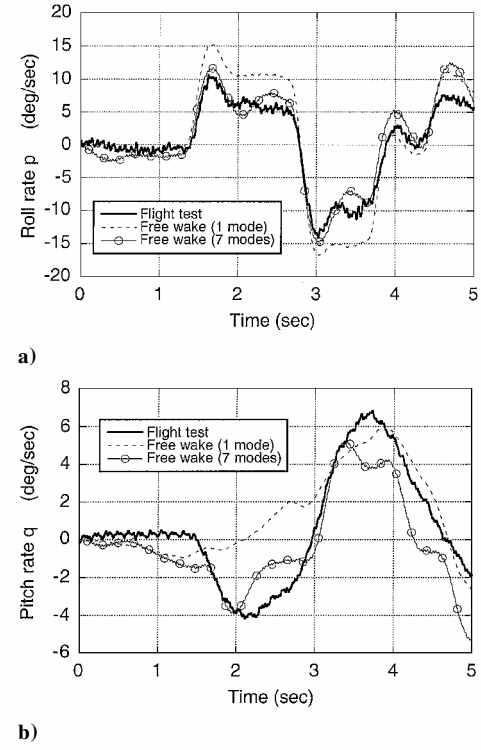

Fig. 8 Effect of number of modes on the a) roll and b) pitch rate response; free wake model.

to the reversal of the lateral cyclic input. Before the application of the first lateral cyclic input, that is, for $t \leq 1.5$ s, the predicted pitch rate response slowly drifts away from zero: This is due to the trim methodology, as mentioned in the preceding section.

The free wake, seven-modes results shown in Fig. 8 are the best results obtained in the present study. In all of the results that follow, one or more modeling features are removed, to study the effect of those features on the accuracy of the predictions.

The other curves in Fig. 8 have been obtained using the simple blade model, that is, representing blade flexibility with just the first flap mode. The on-axis response p tends to be overpredicted, although it remains in phase with the lateral input. The off-axis response q, on the other hand, is predicted poorly: The initial nose-down motion is missed almost completely, and good agreement is recovered only after 3–4 s. Therefore, Fig. 8 suggests that the prediction of the response to pilot inputs is a truly aeroelastic problem

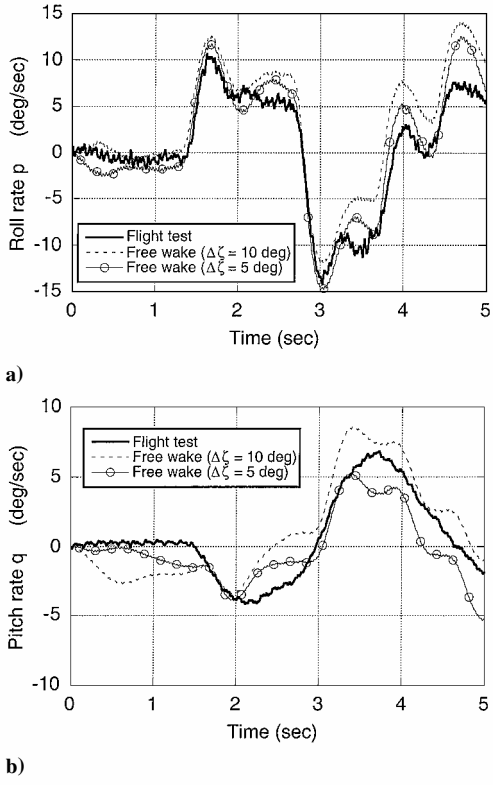

Fig. 9 Effect of the resolution of the free wake vortex filament discretization $\Delta\zeta$ on the a) roll and b) pitch rate response; seven-mode flexible blade model.

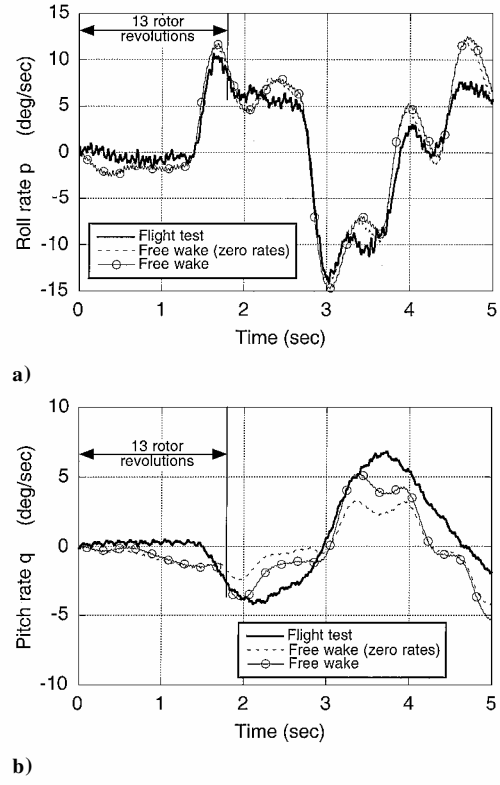

Fig. 10 Effects on the a) roll and b) pitch rate response of modeling the free wake geometry changes due to the maneuver; seven-mode flexible blade model.

that requires a careful modeling of blade flexibility, at least for a highly coupled, hingeless rotor helicopter like the BO-105.

When the free wake model is used in the calculations, the vortex wake is represented by a single vortex filament that is released from the three-quarter-chord location at the blade tip. The vortex filament discretization resolution $\Delta\zeta$ of the wake in Fig. 8 is 5 deg, and the total length of each filament is 720 deg. Figure 9 shows the effect of reducing the free wake vortex filament discretization resolution, that is, increasing $\Delta\zeta$, on the accuracy of the prediction of roll and pitch rate responses. From a computational efficiency point of view, the resolution $\Delta\zeta$ is an important parameter. In fact, by halving $\Delta\zeta$, the computer time required increases more than fourfold. The results shown in Fig. 9 are generated with wake resolutions of $\Delta\zeta = 5$ deg, as in Fig. 8, and $\Delta\zeta = 10$ deg. The refined, seven-mode blade model is used for both cases. The roll rate p is predicted well using both vortex wake resolutions, with the finer resolution providing a slightly better accuracy. For the pitch rate q predictions, the coarser discretization still gives reasonably good results, but the finer discretization is noticeably more accurate. As to the total length of each filament, results were also obtained with lengths greater than 720 deg: The results were generally so close to those obtained with a 720-deg length that they have not been included in the present paper.

The free wake used in this study is capable of modeling the changes in wake geometry caused by the maneuver.[12] Figure 10 attempts to separate the effects of these maneuver-induced changes on the pitch and roll rate predictions. The seven-mode blade model is used. Wake resolution and maximum wake age are the same as in Fig. 8, that is, $\Delta\zeta = 5$ deg, and the total length of each filament is 720 deg. The "Free wake (zero rates)" legend indicates the results obtained by arbitrarily setting to zero the roll and pitch rates provided to the free wake as inputs; although not completely rigorous, this effectively removes the maneuvering effects from the free wake model. Roll and pitch rates are set to zero only for the calculation of the free wake geometry; in all of the other portions of the model, p and q retain their correct value. Figure 10 shows that the roll rate response p is not significantly affected. On the other hand, there is some worsening of the off-axis correlation, and the magnitude of the pitch response tends to be underpredicted. Therefore, the changes in wake geometry due to the maneuver need to be taken into account for a good prediction of the off-axis response, although they do not appear to be important for the on-axis predictions.

The time corresponding to the 13th rotor revolution is marked on the plots in Fig. 10. This is close to the time at which the highest values of the roll and pitch rates are reached following the initial lateral cyclic control input. The inclusion of maneuvering effects on the free wake geometry should be most visible at this time. Recall that in the simulation of a given rotor revolution the wake geometry, and associated inflow distribution, is that obtained from the previous rotor revolution and is held fixed through the current rotor revolution.

Figures 11a and 11b show, respectively, a rear and side view of the wake geometry during the 13th rotor revolution into the maneuver. The x and z coordinates are normalized with respect to the rotor radius. The roll and pitch rates are about 9 and 3 deg/s respectively. The thin lines in Figs. 11 show the geometry of the wake with the maneuvering effects removed by setting $p = q = 0$. The thick lines show the geometry of the wake with the free wake maneuvering effects correctly modeled. A small amount of wake rollup becomes visible near the end of the wake on both the advancing and retreating sides of the disk, even at this near hover flight condition of 17 kn. The geometries of two wakes are very similar. There is a small contraction of the wake on the advancing side, that is, the vortices are closer together, and there is elongation on the retreating side due to the inclusion of the positive (advancing side down) roll rate on the wake geometry. This similarity of the wake geometries with and without maneuvering effects is not surprising, considering that the values of the roll and pitch rates are themselves quite small. However, the differences in the pitch rate response (Fig. 10), with and without the maneuvering effects, show that even this small difference in the wake geometries can have a noticeable effect on the off-axis response prediction.

Figure 12 shows the perturbation in inflow from the wake geometry changes resulting from the inclusion of maneuvering effects.

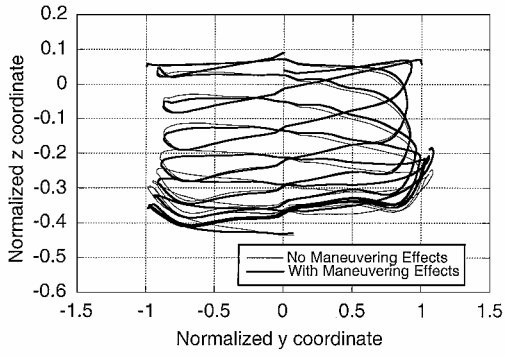

a) Rear view

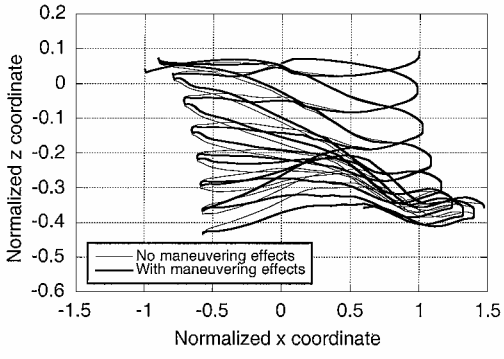

b) Side view

Fig. 11 Free wake geometry with and without maneuvering effects, 13 rotor revolutions after the start of the simulation.

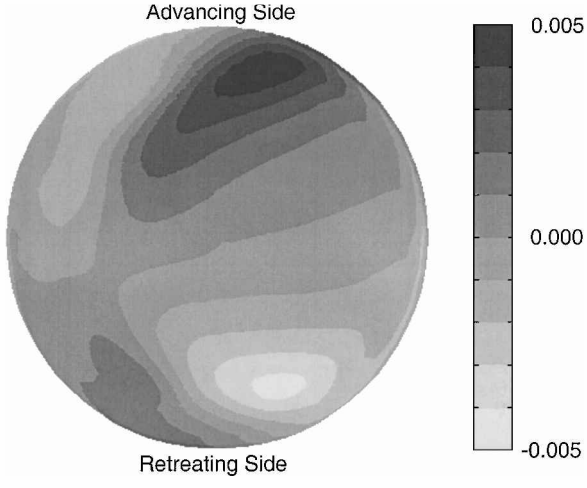

Fig. 12 Difference in nondimensional inflow between free wake model with and without maneuver effects at 13 rotor revolutions; no maneuver effects is the baseline.

This perturbation is defined as the inflow distribution generated with the maneuvering effects included, minus the inflow distribution that does not include those effects. This essentially isolates the effects of maneuver-induced changes in wake geometry on the inflow distribution. However, note that, because p and q are set to zero only for the calculation of the wake distortion due to the maneuver and nowhere else, the changes in inflow due to the kinematics of the maneuver are still retained in both cases. For example, in both cases a nose-up pitching motion of the helicopter will generate a downward flow on the front of the disk (and, therefore, a decrease in the local angle of attack of the blade) and an upward flow on the rear (with an increase in angle of attack).

The inflow perturbation just defined, and shown in Fig. 12, essentially corresponds to an additional downwash on the advancing side and an additional upwash on the retreating side. This translates into lower angles of attack, lower lift, and lower flapping moments on the advancing side; with the reverse being true on the retreating side. Because of the delay in the flapping response of the rotor, this in turn translates into an increase in longitudinal flapping (tip path plane tilting down over the nose) and helps explain the stronger nose-down pitch rate achieved at this point in the time history calculations with the maneuver-induced wake distortions included (See Fig. 10).

Comparison with Keller's[3] Extended Dynamic Inflow Model

The other inflow model that is investigated in this study is an extended momentum theory model, proposed by Keller,[3] which includes additional inflow terms proportional to pitch and roll rates. This model is characterized by a wake distortion parameter K_R that is determined based on a simplified vortex wake analysis (or may be identified from flight-test data). The value proposed by Keller for hover was 1.5. Other studies have determined different values for this parameter, from 0.75 to 1.75 (Ref. 6) with the specific values depending on the theory used. Figure 13 compares results obtained using various values of the wake distortion parameter K_R with results obtained with the dynamic inflow model and with flight-test data. The dynamic inflow results can be considered as the case $K_R = 0$. The seven-mode refined blade model was used. The modification to the dynamic inflow model proposed by Keller[3] is strictly only valid in the hover flight condition; here it is used in a near hover flight condition, that is, 17 kn. Figure 13 shows that the on-axis roll rate response p is not significantly changed with the inclusion of the wake distortion effects. On the other hand, the off-axis correlation is noticeably improved with the addition of the wake distortion effects. The best overall correlation among the various values of K_R seems to occur for $K_R = 1.5$.

Finally, Fig. 14 compares the results obtained with the maneuvering free wake model and with the extended dynamic inflow and $K_R = 1.5$. Both results are generated with the seven-mode refined blade model. The on-axis roll rate response is predicted with good accuracy with both inflow models. The free wake model predicts the off-axis pitch rate response more accurately. Keller's model,[3] as a linear inflow model, cannot be used for the prediction of vibratory loads; however, it does capture the main features of the off-axis response and is computationally far more efficient than the

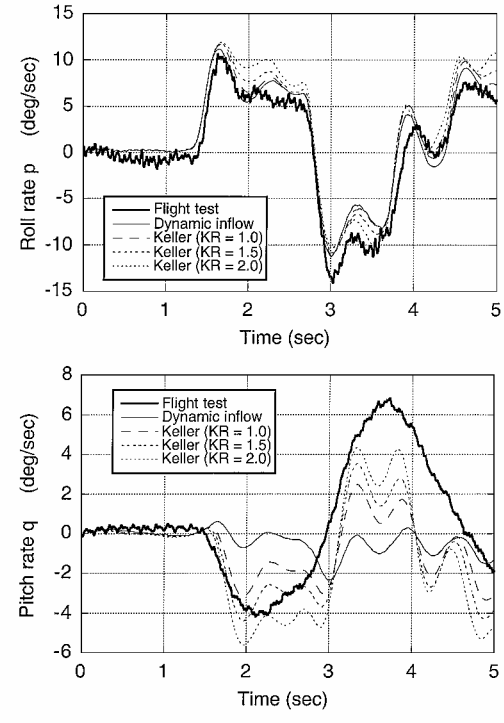

Fig. 13 Effect of wake distortion parameter K_R; seven-mode blade model.

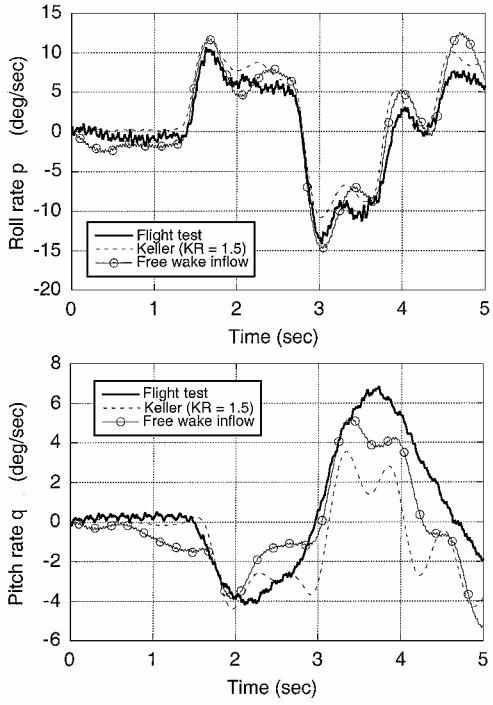

Fig. 14 Comparison of response with maneuvering free wake model and extended dynamic inflow model with $K_R = 1.5$; seven-mode blade model.

free wake model. (Compared with the free wake model, the overall CPU time required for the simulation is 10% or less.) Therefore, for typical flight dynamic simulations, using an extended dynamic inflow model such as Keller's, with the K_R constant calibrated using a more accurate maneuvering free wake model, appears to be the most cost-effective strategy.

Conclusions

A coupled rotor–fuselage flight dynamic model that includes a maneuvering free wake model and a coupled flap–lag–torsion flexible blade model has been developed to investigate some effects of inflow and blade modeling on the free-flight response to pilot inputs of a hingeless rotor helicopter. The wake model is a relaxation type free wake, capable of modeling the wake geometry changes due to maneuvers; no assumptions are made on the wake geometry, which is free to evolve based on the maneuver. Theoretical predictions were compared with flight-test data.

A series of factors needs to be carefully taken into account when evaluating the conclusions of this study. The study focused on a single maneuver, conducted in near hover conditions. The amplitude of the inputs was relatively small, and the helicopter response was mostly in a linear range. Through the incorporation of the maneuvering free wake it was possible to obtain realistic values of the vibratory loads, but no vibratory load validation was carried out. The helicopter considered in the study was a high equivalent hinge offset, highly coupled configuration, and, therefore, it can almost be considered as a worst-case scenario from the point of view of predicting pitch–roll cross couplings. With this in mind, the main conclusions are as follows:

1) The maneuvering free wake used in this study can be effectively used in free-flight response simulations, even if it is rigorously valid only for steady, trimmed conditions.

2) The trim calculations must be carried out much more accurately when a free wake model, rather than a dynamic inflow type model is used. Many more harmonics of rotor blade motion are likely to be needed for a harmonic balance type, algebraic trim procedure. A shooting type procedure that explicitly enforces periodicity of rotor and fuselage states may prove necessary.

3) The free-flight, on-axis response to pilot pitch and roll inputs can be predicted with good accuracy with a relatively unsophisticated model; neither a free wake nor a refined flexible blade model are required.

4) It is possible to predict the off-axis response from first principles, that is, without empirically derived correction factors and without assumptions on the wake geometry. To do so, however, requires sophisticated modeling. Both a free wake model that includes the wake distortions caused by the maneuver and a refined flexible blade model must be used.

5) Most features of the off-axis response can be captured using a dynamic inflow theory extended to account for maneuver-induced wake distortions, for a fraction of the cost of using a free wake model. The most cost-effective strategy, for typical flight dynamic analyses and if vibratory loads are not required, is probably to calibrate such a theory using the more accurate free wake based model and then use it in all calculations.

Acknowledgments

This research was supported by the National Rotorcraft Technology Center under the Rotorcraft Center of Excellence program. The authors would like to thank A. Bagai and J. G. Leishman for providing a copy of the maneuvering free wake code and for many useful discussions. Detailed configuration parameters for the BO-105 were provided by A. Desopper of ONERA, France. Flight-test data for the BO-105 were provided by C. Ockier of DLR, Germany.

References

[1] Rosen, A., and Isser, A., "A New Model of Rotor Dynamics During Pitch and Roll of a Hovering Helicopter," *Journal of the American Helicopter Society*, Vol. 40, No. 3, 1995, pp. 17–28.

[2] Rosen, A., and Isser, A., "A Model of the Unsteady Aerodynamics of a Hovering Rotor that Includes Variations of the Wake Geometry," *Journal of the American Helicopter Society*, Vol. 40, No. 3, 1995, pp. 6–16.

[3] Keller, J. D., "An Investigation of Helicopter Dynamic Coupling Using an Analytical Model," *Journal of the American Helicopter Society*, Vol. 41, No. 4, 1996, pp. 322–330.

[4] Keller, J. D., and Curtiss, H. C., Jr., "A Critical Examination of the Methods to Improve the Off-Axis Response Prediction of Helicopters," *Proceedings of the 54th Annual Forum of the American Helicopter Society*, Washington, DC, May 1998.

[5] Arnold, U. T. P., Keller, J. D., Curtiss, H. C., and Reichert, G., "The Effect of Inflow Models on the Predicted Response of Helicopters," *Journal of the American Helicopter Society*, Vol. 43, No. 1, 1998, pp. 25–36.

[6] Basset, P.-M., and Tchen-Fo, F., "Study of the Rotor Wake Distortion Effects on the Helicopter Pitch-Roll Cross-Coupling," *Proceedings of the 24th European Rotorcraft Forum*, Marseilles, France, Sept. 1998.

[7] Krothapalli, K. R., Prasad, J. V. R., and Peters, D. A., "Improved Wake Geometry for a Maneuvering Rotor," *Proceedings of the AHS Technical Specialists' Meeting for Rotorcraft Acoustics and Aerodynamics*, Williamsburg, VA, Oct. 1997.

[8] Krothapalli, K. R., Prasad, J. V. R., and Peters, D. A., "A Generalized Dynamic Wake Model with Wake Distortion Effects," *Proceedings of the 54th Annual Forum of the American Helicopter Society*, Washington, DC, May 1998.

[9] von Grünhagen, W., "Dynamic Inflow Modeling for Helicopter Rotors and Its Influence on the Prediction of Crosscoupling," *Proceedings of the American Helicopter Society Aeromechanical Specialists' Conference*, Fairfield County, CT, Oct. 1995.

[10] Mansur, M. H., and Tischler, M. B., "An Empirical Correlation Method for Improving Off-Axis Response in Flight Mechanics Helicopter Models," *Journal of the American Helicopter Society*, Vol. 43, No. 2, 1998, pp. 94–102.

[11] Rosen, A., Yaffe, R., Mansur, M. H., and Tischler, M. B., "Methods for Improving the Modeling of Rotor Aerodynamics for Flight Mechanics Purposes," *Proceedings of the 54th Annual Forum of the American Helicopter Society*, Washington, DC, May 1998.

[12] Bagai, A., Leishman, J. G., and Park, J., "Aerodynamic Analysis of a Helicopter in Steady Maneuvering Flight Using a Free-Vortex Rotor Wake Model," *Journal of the American Helicopter Society*, Vol. 44, No. 2, 1999, pp. 109–120.

[13] Park, J. S., and Leishman, J. G., "Investigation of Unsteady Aerodynamics on Rotor Wake Effects in Maneuvering Flight," *Proceedings of the 55th Annual Forum of the American Helicopter Society*, Montréal, Canada, May 1999.

[14] Kim, F. D., Celi, R., and Tischler, M. B., "High-Order State Space Simulation Models of Helicopter Flight Mechanics," *Journal of the American Helicopter Society*, Vol. 38, No. 4, 1993, pp. 16–27.

[15]Turnour, S. R., and Celi, R., "Modeling of Flexible Rotor Blades for Helicopter Flight Dynamics Applications," *Journal of the American Helicopter Society*, Vol. 41, No. 1, 1996, pp. 52–66; correction in Vol. 41, No. 3, 1996, pp. 191–194.

[16]Turnour, S. R., and Celi, R., "Effect of Unsteady Aerodynamics on the Flight Dynamics of an Articulated Rotor Helicopter," *Journal of Aircraft*, Vol. 34, No. 2, 1997, pp. 187–196.

[17]Peters, D. A., and HaQuang, N., "Dynamic Inflow for Practical Applications," *Journal of the American Helicopter Society*, Vol. 33, No. 4, 1988, pp. 64–68.

[18]Bagai, A., and Leishman, J. G., "Rotor Free-Wake Modeling Using a Pseudo-Implicit Technique—Including Comparison with Experimental Data," *Journal of the American Helicopter Society*, Vol. 40, No. 3, 1995, pp. 29–41.

[19]Theodore, C. R., "Flight Dynamic Modeling of Articulated and Hingeless Rotor Helicopters Including a Refined Aerodynamic Model," Ph.D. Dissertation, Dept. of Aerospace Engineering, Univ. of Maryland, College Park, MD, May 2000.

[20]Celi, R., "Helicopter Rotor Dynamics in Coordinated Turns," *Journal of the American Helicopter Society*, Vol. 36, No. 4, 1991, pp. 39–47.

[21]Kim, F. D., Celi, R., and Tischler, M. B., "Forward Flight Trim Calculation and Frequency Response Validation of a High-Order Helicopter Simulation Model," *Journal of Aircraft*, Vol. 30, No. 6, 1993, pp. 854–863.

[22]Chen, R. T. N., and Jeske, J. A., "Kinematic Properties of the Helicopter in Coordinated Turns," NASA TP 1773, April 1981.

[23]Theodore, C. R., and Celi, R., "Prediction of the Off-Axis Response to Cyclic Pitch Using a Maneuvering Free Wake Model," *Proceedings of the 25th European Rotorcraft Forum*, Rome, Italy, Sept. 1999.

[24]Hansford, R. E., and Vorwald, J., "Dynamics Workgroup on Rotor Vibratory Loads Prediction," *Journal of the American Helicopter Society*, Vol. 43, No. 1, 1998, pp. 76–87.

[25]Staley, J. A., "Validation of Rotorcraft Flight Simulation Program Through Correlation with Flight Data for Soft-In-Plane Hingeless Rotors," U.S. Army Air Mobility Research and Development Lab., USAAMRDL-TR-75-50, Jan. 1976.

[26]Kaletka, J., and Gimonet, B., "Identification of Extended Models from BO-105 Flight Test Data for Hover Flight Condition," *Proceedings of the 21st European Rotorcraft Forum*, Saint-Petersburg, Russia, Aug. 1995.